Published in final edited form as:

J Phys Chem Lett. 2015 April 16; 6(8): 1310–1315. doi:10.1021/acs.jpclett.5b00326.

Characterization of Parallel β-sheets at Interfaces by Chiral Sum Frequency Generation Spectroscopy

Li Fu[#,*], **Zhuguang Wang**, **Brian T. Psciuk**, **Dequan Xiao**[†], **Victor S. Batista**, and **Elsa C.Y. Yan**[*]

Department of Chemistry, Yale University, 225 Prospect Street, New Haven, CT 06520

Abstract

Characterization of protein secondary structures at interfaces is still challenging due to the limitations of surface-selective optical techniques. Here, we address the challenge of characterizing parallel β-sheets by combining chiral sum frequency generation (SFG) spectroscopy and computational modeling. We focus on human islet amyloid polypeptide aggregates and a *de novo* designed short polypeptide on at lipid/water and air/glass interfaces. We find that parallel β-sheets adopt distinct orientations at various interfaces and exhibit characteristic chiroptical responses in the amide I, and N-H stretch regions. Theoretical analysis indicates that the characteristic chiroptical responses provide valuable information on the parallel β-sheet symmetry, orientation and vibrational couplings at interfaces.

Graphical abstract

[*]**Corresponding Authors:** Tel: (203) 436-2509. Fax: (203) 432-6144. elsa.yan@yale.edu, Tel: (509) 371-6755. li.fu@pnnl.gov.
[†]Current Address: Department of Chemistry and Chemical Engineering, University of New Haven, West Haven, CT 06516
[#]Current Address: William R. Wiley Environment Molecular Sciences Laboratory, Pacific Northwest National Laboratory, P.O. Box 999, Richland, WA 99352, U.S.A.

Supporting Information: Materials and methods. Experimental SFG spectrometer. Intensity ratio of amide I B to amide I A mode in the *psp* spectrum as a function of twist angle (ψ). Spectral parameters obtained by fitting the amide I bands in Figure 3. The *ssp* SFG spectrum of peptide 1 at the glass slide surface. Derivation of the effective susceptibility as a function of hyperpolarizability elements (including the *ssp* SFG spectrum of hIAPP aggregates at the lipid/water and the air/glass interfaces). Contribution of turn structures to the ~1660 cm^{-1} peak in hIAPP spectra. Characterization of peptide 1. This material is available free of charge via the Internet at http://pubs.acs.org.

Notes

The authors declare no competing financial interest.

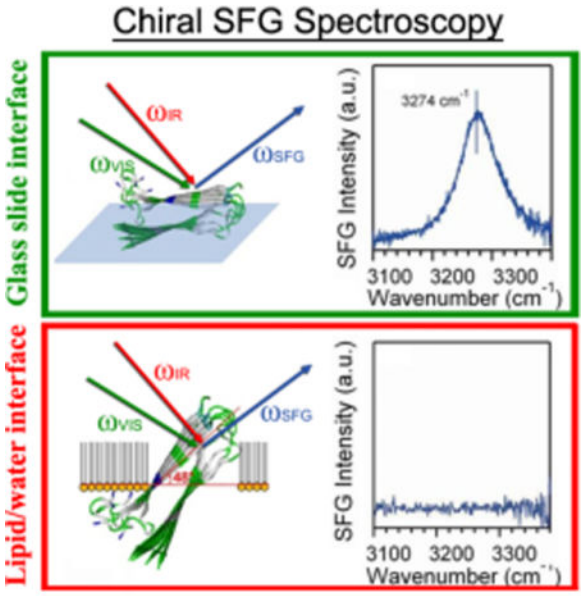

Keywords

amylin; human islet amyloid polypeptide; orientation; *ab initio* calculation; vibrational spectroscopy

Assembly of parallel β-sheets at interfaces is critical for the design of ordered chiral macromolecular architectures[1] and for understanding structure/function relations in amyloid aggregates.[2–3] The assembly occurs at aqueous interfaces of various materials, such as lipid membranes or biosensors, which could be remarkably different from that occurs in the bulk solutions. Using conventional characterization techniques such as Fourier transform infrared (FTIR), Raman, and circular dichroism (CD) spectroscopy, it is often difficult to obtain information about protein secondary structures exclusively at the interface, while simultaneously eliminate the interference from background of molecules such as lipid and water. Therefore, there is a need to develop surface-selective optical techniques for characterization macromolecular structures at interfaces.

In recent years, sum frequency generation (SFG) spectroscopy has gained increasing attention as applied to studies of proteins,[4–13] DNAs,[14–17] and other biomolecules.[18–22] SFG is often sensitive to the interfacial contributions and is background free from the bulk solution,[23] allowing for studies of molecular structure, orientation and dynamics at interfaces. In addition, SFG can selectively probe chirality that is gaining tremendous attentions in probing biomolecules by nonlinear optics such as SFG.[24–25] We have applied chiral SFG by probing the N-H stretch and amide I bands to distinguish protein secondary structures.[26–28] We have monitored, *in situ* and in real time, the misfolding of human islet amyloid polypeptide (hIAPP) into parallel β-sheets via an α-helical intermediate at the lipid/water interface,[26, 28–29] and proton exchange in parallel β–sheets at interfaces.[30] We have also demonstrated that chiral SFG can be used to determine the orientation of the parallel β-strand of hIAPP aggregates at interfaces by analyzing the chiral amide I spectrum.[28, 31–32]

Nonetheless, rigorous testing of theoretical descriptions about chiral SFG response of macromolecules using experimental data under various conditions are still scarce, but much is needed to move the SFG field forward particularly for applications in biological and material sciences. Here, we use parallel β-sheet as a model to demonstrate the synergic approach of combining theory and experiments to analyze the chiral and achiral SFG response of parallel β-sheet, constructing a framework for further developments of theoretical and experimental approaches for analyzing other protein secondary structures, such as anti-parallel β-sheet, α–helix, and 3_{10}-helix, and even beyond protein secondary structures, such as DNA and polysaccharide.

We use hIAPP aggregates as well as a *de novo* designed short peptide (**peptide 1**) as model systems. The hIAPP is a 37-amino acid peptide hormone, secreted by human pancreatic β-cells, which forms parallel β-sheet amyloid aggregates upon interactions with negatively charged lipid molecules.[33] The peptide 1 (Scheme 1), developed by Gellman and coworkers, has a D-proline amino acid linker confining two β-strands into a parallel β-sheet structure.[34]

We combine experiments and theoretical modeling to obtain the chiral SFG spectra of both the N-H stretch and amide I regions and we show that the chiral optical responses of parallel β-sheets are determined by three factors, including the molecular symmetry, vibrational coupling, and the molecular orientation at interfaces. Our analysis in agreement with the SFG spectra simulated by using the molecular hyperpolarizability calculated by *ab initio* quantum chemistry methods. Our results illustrate a quantitative approach for analyzing SFG spectra to extract information about structures, orientation, and vibrational coupling of parallel β-sheet structures at interfaces which should be useful for studies of other macromolecular structures at interfaces.

Figure 1 shows the chiral SFG spectra of hIAPP aggregates at the lipid/water interface and at the air/glass surface in the amide I and N-H stretch vibrational regions. The peak intensities and positions of the bands, shown in Table 1, were obtained by fitting the spectra to the Lorentzian function:

$$I_{SFG} \propto \left| \chi_{NR}^{(2)} + \sum_q \frac{A_q}{\omega_{IR} - \omega_q + i\Gamma} \right|^2 \quad (1)$$

where I_{SFG} is the sum frequency intensity, $\chi_{NR}^{(2)}$ is the nonresonant second-order susceptibility,[35] ω_{IR} is the incident IR frequency, and A_q, ω_q, and Γ_q are the amplitude, resonant frequency, damping factor of the qth vibration mode, respectively.

Figure 1 shows that hIAPP aggregates exhibit a significantly different chiral optical response when probed at the lipid/water interface, or on a glass slide. The chiral amide I band of hIAPP at the lipid/water interface shows a peak at 1622 cm^{-1} and a shoulder at 1660 cm^{-1} (Figure 1A), assigned to the B (asymmetric stretch) and A (symmetric stretch) modes, respectively, of the amide I band (Scheme 2).[36–37] On the glass slide, the peak is at 1621 cm^{-1} (B mode) and the shoulder at 1667 cm^{-1} (A mode) (Figure 1B). Although turn structures

have characteristic amide I vibrational frequency also at ~1660 cm^{-1}, the contribution should be negligible according to the low surface population in the hIAPP structures and previous reports in literature[38] (see Supporting Information). Thus, as an approximation, we neglect the contribution from β-turns and only consider contribution from the amide I *A* mode to the ~1660 cm^{-1} peak. The intensity ratio of the *B* mode (~1620 cm^{-1}) relative to the *A* mode (~1660 cm^{-1}) is much smaller than the ratio for the aggregates at the lipid/water interface (Figure 1A). More dramatic differences are observed for the N-H stretch spectra, showing a peak at 3301 cm^{-1} on the glass slide (Figure 1B) but no signal at the lipid/water interface (Figure 1A).

The observed differences in the SFG chiral optical response of hIAPP in different spectral regions at various interfaces raise an important question: what determines the selectivity of the SFG response of the parallel *β*-sheet structure at the interface? We address this question by considering three factors: (1) molecular symmetry, (2) vibrational coupling, and (3) molecular orientation.

Molecular Symmetry

Molecular symmetry governs the chiroptical responses of interfacial molecules through the hyperpolarizability elements.[39] While a single amide group has C_s symmetry, the chiral SFG response originates from the macroscopic arrangement of multiple amide I groups in protein backbones, and thus should conform to the symmetry of the secondary structure under study. The parallel *β*-sheet in our study adopts a C_2 symmetry, giving the following non-zero hyperpolarizability tensor elements: $\beta_{abc}=\beta_{bac}$, $\beta_{cba}=\beta_{bca}$, $\beta_{acb}=\beta_{cab}$, $\beta_{cbc}=\beta_{bcc}$, $\beta_{aba}=\beta_{baa}$, β_{bbb}, β_{ccb}, β_{aab}, with the molecular coordinates (*a*, *b*, *c*) defined in Scheme 3. Using these nonzero hyperpolarizability elements, one can express the effective susceptibility of SFG in the *psp* polarization setting (see Supporting Information for derivation):

$$\chi^{(2)}_{psp,q} = -\frac{L_{zyx}}{2}N_S\begin{Bmatrix}\langle\cos^2\theta\rangle(\beta_{cab}-\beta_{cba})+\langle\sin^2\theta\sin^2\psi\rangle(\beta_{bca}-\beta_{bac})\\+\langle\sin^2\theta\cos^2\psi\rangle(\beta_{acb}+\beta_{abc})\\+\langle\sin\theta\cos\theta\cos\psi\rangle(-\beta_{aab}+\beta_{aba}-\beta_{cbc}+\beta_{ccb})\end{Bmatrix} \quad (2)$$

, where θ is the tilt angle between the *c*-axis of the *β*-sheet and the interface, while ψ is the twist angle between the *b*-axis of the *β*-sheet and the interface (Scheme 3), N_s is the surface population, and L_{zyx} is the Fresnel factor. Equation (2) serves as a basis for quantitative interpretation of the chiral SFG spectra of the parallel *β*-sheet.

Vibrational Coupling

The hyperpolarizability elements of the complete parallel *β*-sheet can be obtained by summation of the contributions of individual amide groups since the N-H stretch modes are typically localized without significant coupling.[40] Thus, Eq. (2) can be directly applied to describe the chiral N-H signal based on their spatial arrangement of amide groups along the polypeptide backbone.[39] In contrast, the amide I modes of parallel *β*-sheets are coupled and

split into two bands corresponding to the antisymmetric A and symmetric B vibrational modes (Scheme 2).[37]

According to group theory, the elements β_{aab}, β_{ccb}, $\beta_{acb} = \beta_{cab}$, and β_{bbb} are associated with the A mode, while the associated with the elements $\beta_{abc} = \beta_{bac}$ $\beta_{cbc} = \beta_{bcc}$ $\beta_{cba} = \beta_{bca}$ $\beta_{aba} = \beta_{baa}$ are associated with the B mode. Thus, one can rewrite Eq. (2) to describe the A and B modes, as follows:

$$\chi^{(2)}_{psp,A} = -\frac{L_{zyx}}{2}N_S\left\{\left\langle\cos^2\theta\right\rangle\beta_{cab} - \left\langle\sin^2\theta\cos^2\psi\right\rangle\beta_{acb} + \langle\sin\theta\cos\theta\cos\psi\rangle(\beta_{ccb} - \beta_{aab})\right\} \quad (3)$$

.

$$\chi^{(2)}_{psp,B} = -\frac{L_{zyx}}{2}N_S\left\{\begin{array}{c} -\left\langle\cos^2\theta\right\rangle\beta_{cba} + \left\langle\sin^2\theta\sin^2\psi\right\rangle(\beta_{bca} - \beta_{bac}) \\ +\left\langle\sin^2\theta\cos^2\psi\right\rangle\beta_{abc} + \langle\sin\theta\cos\theta\cos\psi\rangle(\beta_{aba} - \beta_{cbc}) \end{array}\right\} \quad (4)$$

.

Hence, while the N-H stretch of parallel β-sheets can be described by Eq. (2), the A mode and B modes of the amide I vibrations are described by Eqs. (3) and (4), respectively.

Orientation

The effect of orientation is analyzed by using Eqs. (2)–(4). The B mode (1620 cm^{-1}) does not appear in the achiral *ssp* SFG spectra (Figures S3),[31] suggesting that its corresponding transition dipole (Scheme 2) along the c-axis of the β-strands is isotropic (*i.e.*, $\theta = 90°$) at the interface (Scheme 3).

Hence, we can further simplify Eqs. (3) and (4), as follows:

$$\chi^{(2)}_{psp,A} = \frac{L_{zyx}}{2}N_S\left\langle\cos^2\psi\right\rangle\beta_{acb,A} \quad (5)$$

$$\chi^{(2)}_{psp,B} = -\frac{L_{zyx}}{2}N_S\left\{\left\langle\sin^2\psi\right\rangle\beta_{bca,B} + \left(\left\langle\cos^2\psi\right\rangle - \left\langle\sin^2\psi\right\rangle\right)\beta_{bac,B}\right\} \quad (6)$$

Thus, the intensity ratio of B and A modes is a function of the twist angle ψ,[31]

$$I_{\mathrm{B/A}} = \left|\frac{\chi^{(2)}_{psp,B}}{\chi^{(2)}_{psp,A}}\right| = \left|\left\langle\tan^2\psi\right\rangle\frac{\beta_{bca,B}}{\beta_{acb,A}} + \left(1 - \left\langle\tan^2\psi\right\rangle\right)\frac{\beta_{bac,B}}{\beta_{acb,A}}\right|^2. \quad (7)$$

Equation (7), when applied for the chiral amide I signals, can be used to obtain the twist angle ψ of hIAPP aggregates at lipid/water and glass/air interfaces.[31] We obtain the orientation of the hIAPP aggregates (Table 1) giving the observed intensity ratio $I_{B/A} = \left|\frac{A_B/\Gamma_B}{A_A/\Gamma_A}\right|^2$, which is 4.8 for the lipid/water interface (Figure 1A) and 15.9 for the glass slide surface (Figure 1B). In addition, our *ab initio* quantum chemistry calculations yield the tensor elements of $\beta_{bca,B}$, $\beta_{bac,B}$ and $\beta_{acb,A}$ revealing the relationship between intensities and orientation of the parallel β-sheet (ψ) (Figure S1). The tensor elements of $\beta_{bca,B}$, $\beta_{bac,B}$ and $\beta_{acb,A}$ are calculated as in our previous studies,[31–32] using the "divide and conquer" methodology giving $\frac{\beta_{bca,B}}{\beta_{acb,A}} = 1.2$ and $\frac{\beta_{bac,B}}{\beta_{acb,A}} = -3.8$. At the lipid/water interface, $I_{B/A}$=4.8 when the twist angle $\psi \sim 48°$ consistent with our previous analysis.[31] This orientation will bring the hydrophobic β-sheet (white, Figure 1) to the lipid phase and the hydrophilic β-sheet (green, Figure 1) to the water phase; and at the same time, it can position the positively charged arginine residue (blue, Figure 1) right at the level of the negatively charged DPPG lipid head group to facilitate electrostatic interactions. Unlike the *B* mode, whose dipole moment is parallel to the interface, the dipole moment of the *A* mode is nonparallel (Scheme 3) and generates achiral SFG signals at 1660 cm^{-1} in the *ssp* amide I spectra (Figure S3). For the glass slide surface, the achiral *ssp* amide I achiral SFG signals of both the *B* and *A* modes are not observed (Figure S3), suggesting that the average orientation of the dipole moments of both *B* and *A* modes are horizontal (*i.e.*, isotropic on the surface). This indicates that the tilt angle $\theta \sim 90°$ and the twist angle $\psi \sim 0°$. This particular orientation yields a larger intensity ratio of *B* to *A* modes in the chiral *psp* amide I spectrum as predicted by Eq. (7), shown in Figure S1,[31] in agreement with the larger experimentally observed value of $I_{B/A}$=15.9.

The angles θ and ψ define the orientation of parallel β-sheets at lipid/water and glass/air interfaces. For the N-H stretch, the expression of the effective susceptibility given by Eq. (2) can be simplified by setting $\theta = 90°$, as follows:

$$\chi^{(2)}_{psp,N-H\,\text{Stretch}} = -\frac{L_{zyx}}{2}N_S\left\{\left\langle \sin^2\psi\right\rangle\beta_{bca} - \left\langle \cos^2\psi\right\rangle\beta_{acb} + \left\langle \cos^2\psi - \sin^2\psi\right\rangle\beta_{bac}\right\}. \quad (8)$$

The analysis of Eq. (8) shows that the chiral N-H signal can be greatly suppressed, yielding an undetectable signal for hIAPP aggregates at the lipid/water interface. First, a twist angle of ψ=48° is close to 45°, making the term $\langle \cos^2\psi - \sin^2\psi\rangle$ approximately zero. Second, β_{bca} and β_{acb} in Eq. (8) have small contributions to the effective hyperpolarizability $\chi^{(2)}_{psp,N-H\,\text{Stretch}}$ due to the fact that the individual dipole moment of the N-H stretch projects mostly onto the *c*-axis, with a weak projection onto the *a* and *b*-axes (Scheme 2). Previous analysis by Simpson and coworkers supports this argument as they found that, for N-H stretch, β_{bac} ($= -1.91\times10^{-2}$) is about 10 times larger than β_{bca} ($= 6.82\times10^{-4}$) and β_{acb} ($= 1.95\times10^{-3}$).[39] By substituting these values of hyperpolarizability into Eq. (8), we simulated the chiral N-H intensity as a function of orientation for a more quantitative

understanding of the relationship between the chiral N-H stretching signal and the orientation of the parallel β-sheet at the interface (Figure 2).

Figure 2 shows that when the twist (ψ) angle of the parallel β-sheet approaches ~45°, the SFG intensity of N-H stretch vanishes, supporting that the disappearance of the N-H signal of the hIAPP aggregates at the lipid/water interface is due to its orientation with $\psi = 48°$, as revealed from the analysis of the chiral *psp* amide I spectrum. On the other hand, it is expected that the chiral N-H stretching signal can be detected from the hIAPP aggregate, if it adopts an orientation deviated from 45°, as shown in Figure 1B for hIAPP aggregates on a glass surface.

As discussed earlier, the achiral SFG spectra show no noticeable amide I signal from the hIAPP aggregates at the glass slide surface (Figure S3), suggesting that dipole moments of both the A and B modes are parallel to the glass surface and that the hIAPP aggregates are lying flat with the tilt angle $\theta = 90°$ and the twist angle $\psi = 0°$. This indicates that the two β-sheets (upper and lower, Figure 1) in hIAPP adopt an orientation parallel to the surface, presumably with the more hydrophilic sheet (amino acid 28-37) in contact with the glass slide and the more hydrophobic sheet (amino acid 20-27) in contact with the air phase. With such orientation, Eq. (8) predicts that $\chi^{(2)}_{psp,\,N-H\ \mathrm{Stretch}}$ would not be suppressed which is consistent with Figure 2 and with the chiral N-H signal shown in Figure 1B.

To analyze whether the chiral N-H signal is common to other parallel β-sheets, beyond the hIAPP aggregates, we analyzed the SFG spectra of peptide 1 (Scheme 1) in a parallel β-sheet structure.[41] Figure 3 confirms that the chiral N-H stretch signal is observed for peptide 1 with parallel β-sheet with characteristic amide I bands (Figure 3). Two peaks at 1636 cm^{-1} and 1661 cm^{-1} are fitted into Eq. (1) (Table S1) and assigned to the amide I B and A modes, respectively. In addition, we conclude that the long c-axis of peptide 1 aligns with the interface, with $\theta = 90°$, since the achiral amide I SFG spectra is muted (Figure S2). These results agree with our conclusion that the muted chiral N-H stretch spectrum of hIAPP aggregates at the lipid/water interface is due to the specific orientation of hIAPP with ψ close to 45°.

Our analysis thus demonstrates that the chiroptical SFG response from parallel β-sheets is highly dependent on the molecular orientations at the interface. For the amide I spectra, the intensity ratio of the A and B modes can be used to probe the orientation. The intensity of chiral N-H signal also varies with the orientation, and may disappear under specific orientations as observed for hIAPP aggregates.

Conclusions

We have shown how molecular symmetry, vibrational coupling, and molecular orientation determine the chiroptical SFG response from protein secondary structures at interfaces. Our theoretical analysis addresses both amide I and N-H stretching modes for parallel β-sheets at water lipid and air/glass interfaces, and provides a rigorous interpretation of experimental observations. The resulting study of parallel β-sheets clearly demonstrates that the combined theoretical and experimental approach is a valuable methodology for quantitative and

systematic investigation of the chiroptical responses of not only protein secondary structures but also synthetic and native chiral macromolecular structures, such as DNA, RNA, polysaccharides, and supramolecular structures at interfaces. Our work demonstrates the capacity of chiral and achiral SFG for revealing fundamental information about protein structures and orientation at different interfaces, building a foundation for future applications of the method to solve a wide range of problems related to protein structures and functions at interfaces.

Supplementary Material

Refer to Web version on PubMed Central for supplementary material.

Acknowledgments

E.Y. thanks Prof. Samuel Gellman (University of Wisconsin-Madison) for providing the sample of peptide 1, and useful discussions. E.Y. is the recipient of the Starter Grant Award, Spectroscopy Society of Pittsburgh. This work was supported by the National Science Foundation (NSF) grants CHE 1213362 (EY) and CHE-1213742 (VSB), as well as the National Institutes of Health (NIH) grant 1R56DK105381-01 (EY) VSB acknowledges high performance computing time from NERSC. The authors thank Wei Liu for designing the TOC figure. The synthesis of the parallel β-sheet peptide 1 sample carried out by Gellman and coworkers was supported by NIH (R01 GM061238).

References

1. Zhang SG. Fabrication of Novel Biomaterials through Molecular Self-Assembly. Nat Biotechnol. 2003; 21:1171–1178. [PubMed: 14520402]
2. Luca S, Yau WM, Leapman R, Tycko R. Peptide Conformation and Supramolecular Organization in Amylin Fibrils: Constraints from Solid-State Nmr. Biochemistry. 2007; 46:13505–13522. [PubMed: 17979302]
3. DeToma AS, Salamekh S, Ramamoorthy A, Lim MH. Misfolded Proteins in Alzheimer's Disease and Type Ii Diabetes. Chem Soc Rev. 2012; 41:608–621. [PubMed: 21818468]
4. Wang HF, Gan W, Lu R, Rao Y, Wu BH. Quantitative Spectral and Orientational Analysis in Surface Sum Frequency Generation Vibrational Spectroscopy (Sfg-Vs). Int Rev Phys Chem. 2005; 24:191–256.
5. Weidner T, Apte JS, Gamble LJ, Castner DG. Probing the Orientation and Conformation of Alpha-Helix and Beta-Strand Model Peptides on Self-Assembled Monolayers Using Sum Frequency Generation and Nexafs Spectroscopy. Langmuir. 2010; 26:3433–3440. [PubMed: 20175575]
6. Nguyen KT, King JT, Chen Z. Orientation Determination of Interfacial Beta-Sheet Structures in Situ. J Phys Chem B. 2010; 114:8291–8300. [PubMed: 20504035]
7. Kim J, Somorjai GA. Molecular Packing of Lysozyme, Fibrinogen, and Bovine Serum Albumin on Hydrophilic and Hydrophobic Surfaces Studied by Infrared-Visible Sum Frequency Generation and Fluorescence Microscopy. J Am Chem Soc. 2003; 125:3150–3158. [PubMed: 12617683]
8. Nguyen KT, Le Clair SV, Ye SJ, Chen Z. Orientation Determination of Protein Helical Secondary Structures Using Linear and Nonlinear Vibrational Spectroscopy. J Phys Chem B. 2009; 113:12169–12180. [PubMed: 19650636]
9. Somorjai GA, Frei H, Park JY. Advancing the Frontiers in Nanocatalysis, Biointerfaces, and Renewable Energy Conversion by Innovations of Surface Techniques. J Am Chem Soc. 2009; 131:16589–16605. [PubMed: 19919130]
10. Engel MFM, VandenAkker CC, Schleeger M, Velikov KP, Koenderink GH, Bonn M. The Polyphenol Egcg Inhibits Amyloid Formation Less Efficiently at Phospholipid Interfaces Than in Bulk Solution. J Am Chem Soc. 2012; 134:14781–14788. [PubMed: 22889183]

11. vandenAkker CC, Engel MFM, Velikov KP, Bonn M, Koenderink GH. Morphology and Persistence Length of Amyloid Fibrils Are Correlated to Peptide Molecular Structure. J Am Chem Soc. 2011; 133:18030–18033. [PubMed: 21999711]
12. Jena KC, Covert PA, Hall SA, Hore DK. Absolute Orientation of Ester Side Chains on the Pmma Surface. J Phys Chem C. 2011; 115:15570–15574.
13. Roy S, Covert PA, FitzGerald WR, Hore DK. Biomolecular Structure at Solid–Liquid Interfaces as Revealed by Nonlinear Optical Spectroscopy. Chem Rev. 2014; 114:8388–8415. [PubMed: 24405207]
14. Stokes GY, Gibbs-Davis JM, Boman FC, Stepp BR, Condie AG, Nguyen ST, Geiger FM. Making "Sense" of DNA. J Am Chem Soc. 2007; 129:7492–7493. [PubMed: 17521190]
15. Wurpel GWH, Sovago M, Bonn M. Sensitive Probing of DNA Binding to a Cationic Lipid Monolayer. J Am Chem Soc. 2007; 129:8420–+. [PubMed: 17579416]
16. Howell C, Schmidt R, Kurz V, Koelsch P. Sum-Frequency-Generation Spectroscopy of DNA Films in Air and Aqueous Environments. Biointerphases. 2008; 3:Fc47–Fc51. [PubMed: 20408693]
17. Walter SR, Geiger FM. DNA on Stage: Showcasing Oligonucleotides at Surfaces and Interfaces with Second Harmonic and Vibrational Sum Frequency Generation. J Phys Chem Lett. 2010; 1:9–15.
18. Nagahara T, Kisoda K, Harima H, Aida M, Ishibashi TA. Chiral Sum Frequency Spectroscopy of Thin Films of Porphyrin J-Aggregates. J Phys Chem B. 2009; 113:5098–5103. [PubMed: 19309126]
19. Holman J, Ye S, Neivandt DJ, Davies PB. Studying Nanoparticle-Induced Structural Changes within Fatty Acid Multilayer Films Using Sum Frequency Generation Vibrational Spectroscopy. J Am Chem Soc. 2004; 126:14322–14323. [PubMed: 15521729]
20. Kett PJN, Casford MTL, Davies PB. Orientation of Cholesterol in Hybrid Bilayer Membranes Calculated from the Phases of Methyl Resonances in Sum Frequency Generation Spectra. J Chem Phys. 2013; 138
21. Liu J, Conboy JC. Direct Measurement of the Transbilayer Movement of Phospholipids by Sum-Frequency Vibrational Spectroscopy. J Am Chem Soc. 2004; 126:8376–8377. [PubMed: 15237984]
22. Nielsen JT, Bjerring M, Jeppesen MD, Pedersen RO, Pedersen JM, Hein KL, Vosegaard T, Skrydstrup T, Otzen DE, Nielsen NC. Unique Identification of Supramolecular Structures in Amyloid Fibrils by Solid-State Nmr Spectroscopy. Angew Chem Int Edit. 2009; 48:2118–2121.
23. Shen YR. Surface-Properties Probed by 2nd-Harmonic and Sum-Frequency Generation. Nature. 1989; 337:519–525.
24. Simpson GJ. Molecular Origins of the Remarkable Chiral Sensitivity of Second-Order Nonlinear Optics. ChemPhysChem. 2004; 5:1301–1310. [PubMed: 15499846]
25. Haupert LM, Simpson GJ. Chirality in Nonlinear Optics. Annu Rev Phys Chem. 2009; 60:345–365. [PubMed: 19046125]
26. Fu L, Liu J, Yan ECY. Chiral Sum Frequency Generation Spectroscopy for Characterizing Protein Secondary Structures at Interfaces. J Am Chem Soc. 2011; 133:8094–8097. [PubMed: 21534603]
27. Fu L, Wang ZG, Yan ECY. Chiral Vibrational Structures of Proteins at Interfaces Probed by Sum Frequency Generation Spectroscopy. Int J Mol Sci. 2011; 12:9404–9425. [PubMed: 22272140]
28. Yan ECY, Fu L, Wang Z, Liu W. Biological Macromolecules at Interfaces Probed by Chiral Vibrational Sum Frequency Generation Spectroscopy. Chem Rev. 2014; 114:8471–8498. [PubMed: 24785638]
29. Fu L, Ma G, Yan ECY. In Situ Misfolding of Human Islet Amyloid Polypeptide at Interfaces Probed by Vibrational Sum Frequency Generation. J Am Chem Soc. 2010; 132:5405–5412. [PubMed: 20337445]
30. Fu L, Xiao DQ, Wang ZG, Batista VS, Yan ECY. Chiral Sum Frequency Generation for in Situ Probing Proton Exchange in Antiparallel Beta-Sheets at Interfaces. J Am Chem Soc. 2013; 135:3592–3598. [PubMed: 23394622]
31. Xiao DQ, Fu L, Liu J, Batista VS, Yan ECY. Amphiphilic Adsorption of Human Islet Amyloid Polypeptide Aggregates to Lipid/Aqueous Interfaces. J Mol Biol. 2012; 421:537–547. [PubMed: 22210153]

32. Poojari C, Xiao DQ, Batista VS, Strodel B. Membrane Permeation Induced by Aggregates of Human Islet Amyloid Polypeptides. Biophys J. 2013; 105:2323–2332. [PubMed: 24268144]
33. Knight JD, Hebda JA, Miranker AD. Conserved and Cooperative Assembly of Membrane-Bound Alpha-Helical States of Islet Amyloid Polypeptide. Biochemistry. 2006; 45:9496–9508. [PubMed: 16878984]
34. Fisk JD, Gellman SHA. Parallel Beta-Sheet Model System That Folds in Water. J Am Chem Soc. 2001; 123:343–344. [PubMed: 11456526]
35. Lambert AG, Davies PB, Neivandt DJ. Implementing the Theory of Sum Frequency Generation Vibrational Spectroscopy: A Tutorial Review. Appl Spectrosc Rev. 2005; 40:103–145.
36. Tamm LK, Tatulian SA. Infrared Spectroscopy of Proteins and Peptides in Lipid Bilayers. Q Rev Biophys. 1997; 30:365–429. [PubMed: 9634652]
37. Barth A, Zscherp C. What Vibrations Tell Us About Proteins. Q Rev Biophys. 2002; 35:369–430. [PubMed: 12621861]
38. Wang J, Chen XY, Clarke ML, Chen Z. Detection of Chiral Sum Frequency Generation Vibrational Spectra of Proteins and Peptides at Interfaces in Situ. Proc Natl Acad Sci U S A. 2005; 102:4978–4983. [PubMed: 15793004]
39. Perry JM, Moad AJ, Begue NJ, Wampler RD, Simpson GJ. Electronic and Vibrational Second-Order Nonlinear Optical Properties of Protein Secondary Structural Motifs. J Phys Chem B. 2005; 109:20009–20026. [PubMed: 16853586]
40. Hayashi T, Mukamel S. Vibrational-Exciton Couplings for the Amide I, Ii, Iii, and a Modes of Peptides. J Phys Chem B. 2007; 111:11032–11046. [PubMed: 17725341]
41. Fisk JD, Schmitt MA, Gellman SH. Thermodynamic Analysis of Autonomous Parallel B-Sheet Formation in Water. J Am Chem Soc. 2006; 128:7148–7149. [PubMed: 16734453]

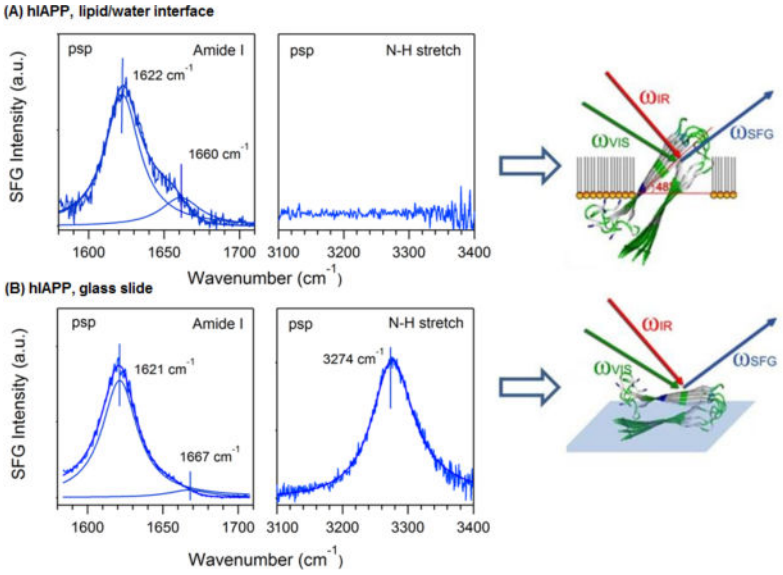

Figure 1.

Chiral *psp* SFG spectra of hIAPP aggregates at interfaces, including the amide I (left) and N-H stretch (right) regions, as well as the orientation of hIAPP aggregates at the (A) lipid/water and (B) air/glass interfaces. Color codes: green for hydrophilic residues, white for hydrophobic residues, and blue for a positively charged arginine residue.

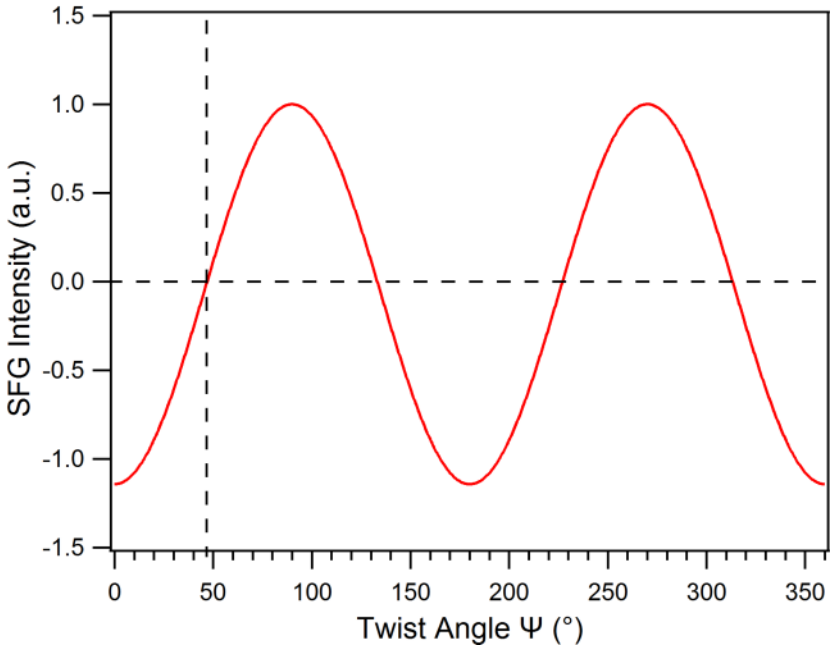

Figure 2.

Simulated SFG intensity of the N-H stretch as a function of ψ, with θ= 90°, using the calculated DFT hyperpolarizability elements.[39]

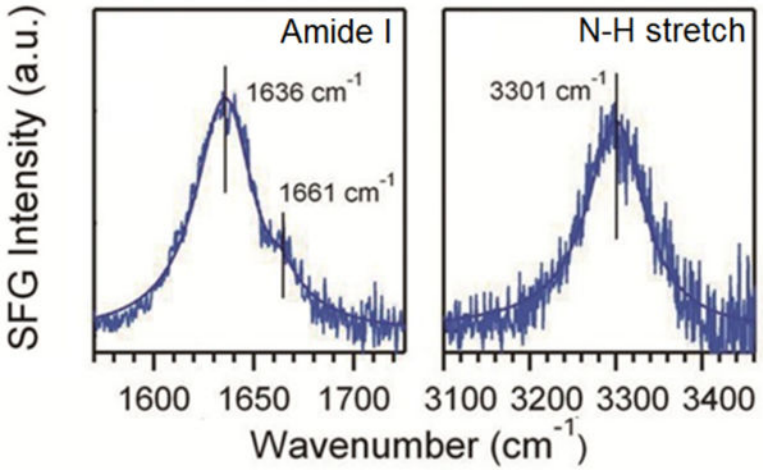

Figure 3.

The *psp* SFG spectra of peptide 1 at the glass slide surface in the amide I and N-H stretch region.

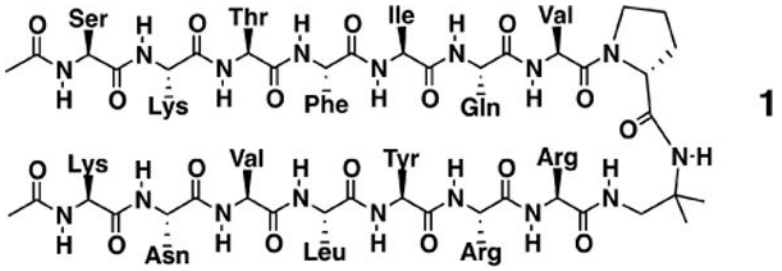

1

Scheme 1.

Peptide 1 with a D-proline amino acid connecting two parallel β-sheet strands.

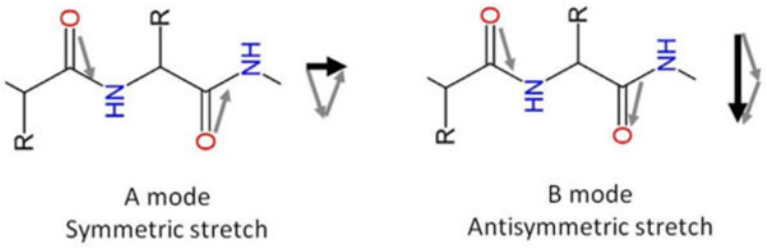

Scheme 2.

A mode and *B* modes of the amide I vibration of parallel *β*-sheets.

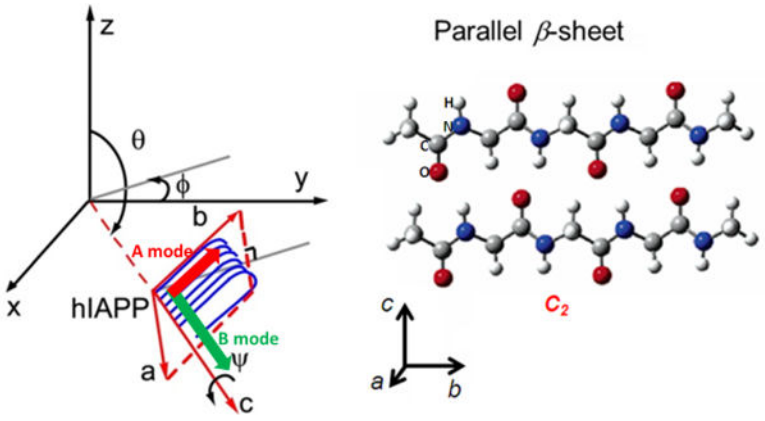

Scheme 3.

Orientation of the β-sheet of hIAPP aggregates with $\theta = 90°$ when the normal to the interface is defined by the z axis.

Table 1

Spectral parameters obtained by fitting the amide I bands, shown in Figure 1.

		hIAPP lipid/water (Figure 1A)	hIAPP glass slide (Figure 1B)
	χ_{NR} (a.u.)	0.02 ± 0.003	−0.189 ± 0.017
A mode	ω_A (cm^{-1})	1660 ± 1.3	1667.4 ± 1.4
	A_A (a.u.)	−2.1 ± 0.16	−8.2 ± 1.1
	Γ_A (a.u.)	16.0 ± 1.1	17.0 ± 1.2
B mode	ω_B (cm^{-1})	1622 ± 1.3	1621 ± 0.1
	A_B (a.u.)	3.9 ± 0.06	27.3 ± 0.2
	Γ_B (a.u.)	13.6 ± 0.3	14.2 ± 0.1